Journal of Statistical Physics, Vol. 37, Nos. 5/6, 1984

Magnetization at Corners in Two-Dimensional Ising Models

Michael N. Barber,[1] Ingo Peschel,[1,3] and Paul A. Pearce[2]

Received June 25, 1984

We investigate the corner spin magnetization of two-dimensional ferromagnetic Ising models in various wedge geometries. Results are obtained for triangular and square lattices by numerical studies on finite wedges using the star–triangle transformation, as well as analytic calculations using corner transfer matrices and a fermionic representation of the row-to-row transfer matrix. The corner magnetizations vanish at the bulk critical temperature T_c with an exponent β_c differing from the bulk exponent. For isotropic systems with free edges we find that β_c is given simply by $\beta_c = \pi/2\theta$, where θ is the angle at the corner. For apex magnetizations of conical lattices we obtain the strikingly similar result $\beta_a = \pi/4\theta$. These formulas apply equally well to anisotropic lattices if the angle θ is interpreted as an effective angle, θ^{eff}, determined by the relative strengths of the interactions.

KEY WORDS: Ising models; corners; magnetization; corner transfer matrices.

1. INTRODUCTION

In a recent paper, Cardy[1] has demonstrated how continuously varying critical exponents can arise on purely geometrical grounds. He studied a magnetic system in d dimensions bounded by two $(d-1)$-dimensional hyperplanes which meet at an angle θ. Adopting a continuum model, he then showed that even within mean field theory critical exponents depend upon

[1] Department of Mathematics, The Faculties, Australian National University, Canberra, A.C.T. 2600, Australia.

[2] Department of Theoretical Physics, Research School of Physical Sciences, Australian National University, Canberra, A.C.T. 2600, Australia.

[3] Permanent address: Fachbereich Physik, Freie Universität Berlin, D-1000 Berlin 33, Germany.

0022-4715/84/1200-0497$03.50/0

822/37/5-6-1

the angle θ. In fact, calculating the spin correlation function at T_c in this approximation corresponds to a well-known electrostatic problem: to find the potential distribution between metallic planes forming a wedge.[2] The exponent η describing the decay (at the bulk critical temperature T_c) of the correlation function between a spin near the edge and one in the interior is then given by $\eta = \pi/\theta$. Similarly, the spontaneous magnetization near the edge varies at T_c with exponent $\beta_c = 1/2 + \pi/2\theta$. This behavior is physically quite plausible since a narrow wedge makes it harder for the system to maintain order, thus leading to a low value of the magnetization.

While Cardy went on to show that these features are maintained in an ε expansion around $d = 4$, we shall in this paper investigate the other interesting situation, $d = 2$. Here the edge becomes a corner and we shall study the behavior of the corner magnetization, m_c, as a function of temperature, angle, lattice structure, and interaction parameters. To do so, three different methods will be used.

We shall first calculate the corner magnetization for finite triangular lattices in the shape of an equilateral triangle with the boundary spins along one edge fixed. The basic technique consists of repeated applications of the star–triangle transformation[3,4] to reduce the lattice to smaller and smaller sizes. This method was introduced by Hilhorst *et al.*[4] in their derivation of an exact renormalization group transformation of the triangular Ising model. More recently, the method has been used to study surface critical behavior in (triangular) Ising models with inhomogeneous couplings near the surface.[5,6]

In our calculation the corner magnetization of the infinite system and, in particular, its critical exponent, is obtained by a finite-size scaling analysis of the finite lattice data. By varying the coupling constants, we can cover various different cases including the square lattices with 45° and 90° corners. We find, indeed, pronounced angle dependence and also in certain cases a dependence on the (spatial) anisotropy of the coupling constants as predicted by Cardy.[1] From the data we are able to conjecture analytical expressions for β_c. These expressions can be further motivated by considering the decay of correlations in *anisotropic* triangular lattices.

Our second method again begins with a triangular lattice but this time wrapped onto a cone. This geometry permits the use of corner transfer matrices,[7] which have proved particularly well suited for magnetization calculations. We find that the properties of such a "conical" system are very similar to those of a system with plane geometry. In particular, the exponent β_a, now referring to the apex magnetization of the cone, shows the same angle dependence.

Finally, in Section 6, we turn to the square lattice with a 90° corner and show how the corner magnetization can be calculated exactly using the conventional row-to-row transfer matrix. To simplify matters, we treat the

problem in the extreme anisotropic (Hamiltonian) limit. The result agrees with the numerical findings.

The paper closes with a summary of our results.

2. CORNER MAGNETIZATION AND STAR–TRIANGLE TRANSFORMATIONS

Consider the triangular lattice as shown in Fig. 1 and label the sites of the lattice by.

$$R = m\mathbf{e}_1 + n\mathbf{e}_2 \equiv (m, n) \tag{2.1}$$

with $m = 0, 1, 2, \ldots, M$, $n = 0, 1, \ldots, m$. The vectors $\mathbf{e}_1$ and $\mathbf{e}_2$ are lattice vectors of the triangular lattice as orientated in Fig. 1. Let the spin at site (m, n) be $\sigma(m, n)$ and set

$$\sigma(M, n) = +1, \qquad n = 0, 1, \ldots, M \tag{2.2}$$

The corner magnetization can be defined by

$$m_c(T) = \lim_{M \to \infty} m_M(T) \tag{2.3}$$

where

$$m_M(T) = \psi'_M(0) \tag{2.4}$$

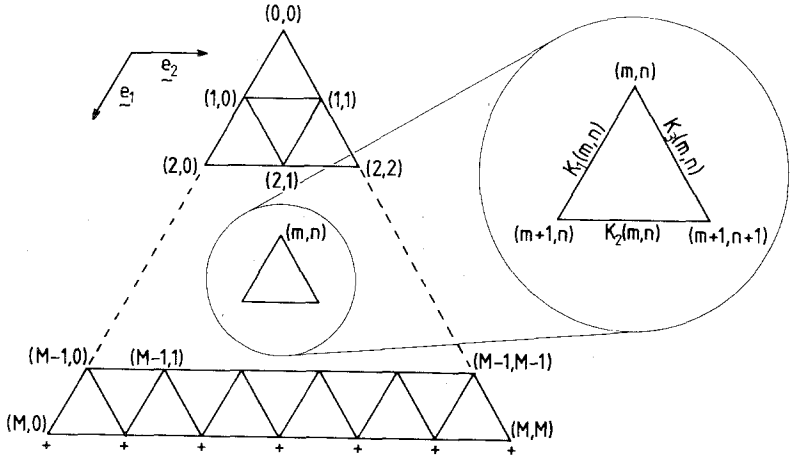

Fig. 1. Geometry of triangular wedge showing orientation of lattice vectors $\mathbf{e}_1$ and $\mathbf{e}_2$, and definition of coupling constants $K_i(m, n)$. Spins along bottom edge of the wedge are frozen, while those along the other edges are free.

with

$$\psi(h) = \ln \sum_{\{\sigma\}} \exp[H_M + h\sigma(0,0)] \tag{2.5}$$

h being a "corner" field coupling only to the spin in the corner. (As usual, we absorb a factor of $-\beta = -1/k_B T$ into the definitions of H_M and h.)

Since our method of evaluating m_M makes the nearest-neigbor interactions of the lattice both anisotropic and spatially dependent even if initially they are homogeneous and isotropic, we consider Hamiltonians of the form

$$\begin{aligned} H_M = \sum_{m=0}^{M} \sum_{n=0}^{m} & [K_1(m,n)\,\sigma(m,n)\,\sigma(m+1,n) \\ & + K_2(m,n)\,\sigma(m+1,n)\,\sigma(m+1,n+1) \\ & + K_3(m,n)\,\sigma(m,n)\,\sigma(m+1,n+1)] \end{aligned} \tag{2.6}$$

Here the interactions around an "up" triangle with "top" vertex at (m, n) are denoted $K_i(m, n)$, $i = 1, 2, 3$, as defined in Fig. 1. Three special cases of (2.6) will be of particular importance:

$$\text{(i)} \quad K_1(m,n) = K_2(m,n) = K_3(m,n) = K \tag{2.7}$$

corresponding to an isotropic triangular lattice with a 60° corner;

$$\text{(ii)} \quad K_1(m,n) = K_3(m,n) = K, \qquad K_2(m,n) = 0 \tag{2.8}$$

corresponding to an isotropic *square* lattice with a 90° corner; and

$$\text{(iii)} \quad K_1(m,n) = K_2(m,n) = K, \qquad K_3(m,n) = 0 \tag{2.9}$$

which is again equivalent to a square lattice but with a 45° corner.

We shall compute $m_M(T)$ iteratively by relating it to the corner magnetization of a lattice of side $M-1$ but with modified couplings. The basic recursion is depicted (for $M = 4$) in Fig. 2. Three steps are involved based upon the star–triangle transformation.[3,4]

We firstly replace all "up" triangles by stars with nodes at the points $(m + 2/3,\ n + 1/3)$. For $0 \leqslant m \leqslant M-2$, the interactions of the star are determined by the interactions of the triangle with "top" vertex at (m, n) and are given by

$$p_i(m,n) = g(K_i(m,n), K_j(m,n), K_k(m,n)) \qquad (i, j, k \text{ cyclic}) \tag{2.10}$$

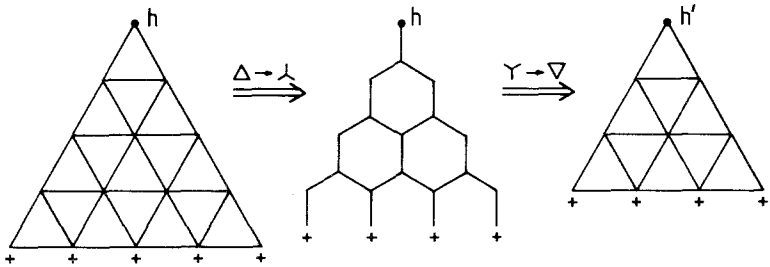

Fig. 2. Reduction of triangular wedge with $M = 4$ spins along each edge to one with $M' = 3$ spins along each edge by use of star–triangle transformations. Note the "corner" field h coupling to the top vertex spin renormalizes to h'.

where $g(K, K', K'')$ is defined in Appendix A. For $m = M - 1$, the transformation simplifies since the last row of spins is frozen. Hence we can set

$$p_2(M-1, n) = K_1(M-1, n) + K_3(M-1, n) \tag{2.11}$$

$n = 0, 1, \ldots, M-1$ and maintain the frozen boundary condition.

At this stage we have a sector of the *hexagonal* lattice (see Fig. 2). We now sum out all spins on the original lattice at sites (m, n) to recover a triangular lattice with spins at sites

$$\mathbf{R}' = m'\mathbf{e}_1 + n'\mathbf{e}_2 = \mathbf{R} - (2\mathbf{e}_1 + \mathbf{e}_2)/3 \tag{2.12}$$

$m' = 0, 1, 2, \ldots, M-1$, $n' = 0, 1, 2, \ldots, m'$, couplings $\{K_i'(m', n')\}$ and a corner field h', the lower boundary again being frozen.

To explicitly determine the transformed couplings K_i' and corner field h' it is convenient to consider three cases.

(*i*) "*Bulk*" *sites—sum over* $\sigma(m,n)$, $1 \leqslant m \leqslant M-1$, $1 \leqslant n \leqslant m-1$. This involves a straightforward application of the star–triangle transformation (see Fig. 3a) and yields

$$\begin{aligned} K_1'(m', n') &= F[p_1(m, n-1), p_2(m+1, n), p_3(m, n)] \\ K_2'(m', n') &= F[p_2(m+2, n+1), p_3(m+1, n+1), p_1(m+1, n)] \\ K_3'(m', n') &= F[p_3(m, n+1), p_1(m, n), p_2(m+1, n+1)] \end{aligned} \tag{2.13}$$

where m' and n' are related to m and n by (2.12) and $F(p, p', p'')$ is defined in (A.1).

(*ii*) "*Left*" *and* "*right*" *edges—sum over* $\sigma(m, 0)$ *and* $\sigma(m, m)$, $m = 1, 2, \ldots, M-2$. These sums involve dedecorations[3] corresponding to degenerate star–triangle transformations with

$$p_1(m, -1) = p_3(m, m+1) = 0 \tag{2.14}$$

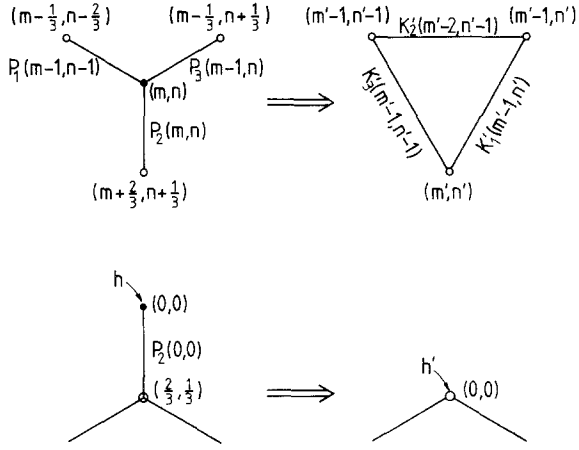

Fig. 3. Schematic representation of the star-to-triangle transformation for (a) an interior site of the hexagonal wedge and (b) the top vertex.

The transformed couplings $K_1'(m', 0)$ and $K_3'(m', m')$ then follow from (2.13) with (2.14) imposed.

(iii) Top corner—sum over $\sigma(0, 0)$. In this case we have explicitly (see Fig. 3b)

$$\sum_{\sigma=\pm 1} \exp\{[h + p_2(0, 0)\mu]\sigma\} = \varphi(h) \exp(h'\mu) \tag{2.15}$$

where $\sigma = \sigma(0, 0)$, μ is the spin at $\mathbf{R}' = (0, 0)$, the top corner of the new lattice,

$$\varphi(h) = \{2[\cosh 2h + \cosh 2p_2(0, 0)]\}^{1/2} \tag{2.16}$$

and

$$h' = \tfrac{1}{2} \ln \left\{ \frac{\cosh[h + p_2(0, 0)]}{\cosh[h - p_2(0, 0)]} \right\} \tag{2.17}$$

The Hamiltonians $H_M = H_M\{K_i(m, m)\}$ and $H_{M-1} = H_{M-1}\{K_i'(m', n')\}$ satisfy

$$\sum_{\{\sigma\}} \exp[H_M + h\sigma(0, 0)] = \varphi(h) e^A \sum_{\{\mu\}} \exp[H_{M-1} + h'\mu(0, 0)] \tag{2.18}$$

where A is independent of h and h'. Hence $\psi_M(h)$ defined by (2.5) satisfies

$$\psi_M(h) = \ln \varphi(h) + A + \psi_{M-1}(h') \tag{2.19}$$

from which we obtain

$$m_M(\{K\}) = \tanh[p_2(0,0)]\, m_{M-1}(\{K'\}) \tag{2.20}$$

This recurrence forms the basis of our analysis of the critical behavior.

Iterating (2.20) gives

$$m_M(\{K_0\}) = \prod_{t=1}^{M} \tanh[p_2^{(t)}(0,0)] \tag{2.21}$$

where the original couplings $\{K_0\}$ are assumed given and $p_2^{(t)}(0,0)$ is the star coupling at site $(0,0)$ generated after t transformations. The iteration terminates when the last triangle is reduced to a single site whose spin is frozen to $\sigma = +1$ by our assumed boundary conditions. [The other solution, $-m_M(\{K\})$, follows if the bottom edge of the lattice is frozen to -1.]

As mentioned in the Introduction our use of the star–triangle transformation is similar to that of Hilhorst *et al.*[4] Indeed, (2.13) become their "star–triangle flow" equations if a continuum limit is taken. They are also a generalization to a more complex geometry of the equations derived by Hilhorst and van Leeuwen[5] to study surface critical behavior in inhomogeneous lattices. As in that case, we can also take a continuum limit

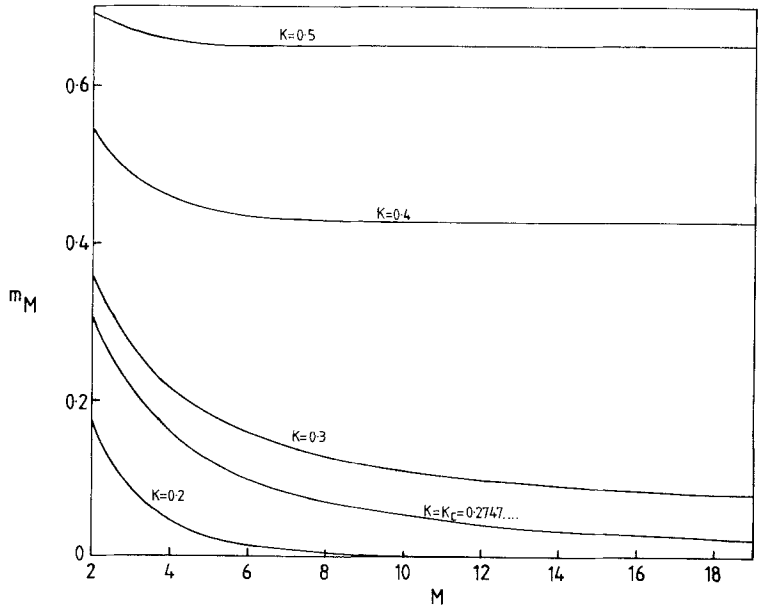

Fig. 4. Convergence of the magnetizations m_M versus M for an isotropic triangular lattice $(K_1 = K_2 = K_3 = K)$ with a 60° corner.

obtaining differential equations for $\partial K_i/\partial t \sim K_i' - K_i$. However, we have been unable to handle these equations because of the complex geometry. Consequently, we shall restrict our attention to *numerical* solutions of the recurrence relations for m_M and numerical extrapolation to obtain m_c and its critical behavior.

For T sufficiently far away from T_c, $m_M(\{K_0\})$ converges rapidly as M increases to a finite nonzero limit for $T < T_c$ and to zero for $T \geqslant T_c$. Figure 4 illustrates the convergence for a 60° corner in an isotropic triangular lattice, the initial couplings K_0 being given by (2.7). As K approaches K_c, the convergence deteriorates but the sequence can be easily accelerated[8] to yield improved limits. Applications of either the u transform of Levin[8,9] or the θ algorithm[8,10] reliably yield estimates of m_c that are accurate to at least three figures for $|T/T_c - 1| \gtrsim 0.01$ given $m_M(T)$ for $M \leqslant 20$. (These accelerators are defined in Appendix B.)

The limiting functions are plotted in Fig. 5 for the three initial sets of coupling constants (2.7)–(2.9), corresponding to corners of 60°, 90°, and 45°, respectively, on isotropic lattices. For comparison, we also show the surface magnetization for an isotropic square lattice[11] corresponding to a 180° corner.

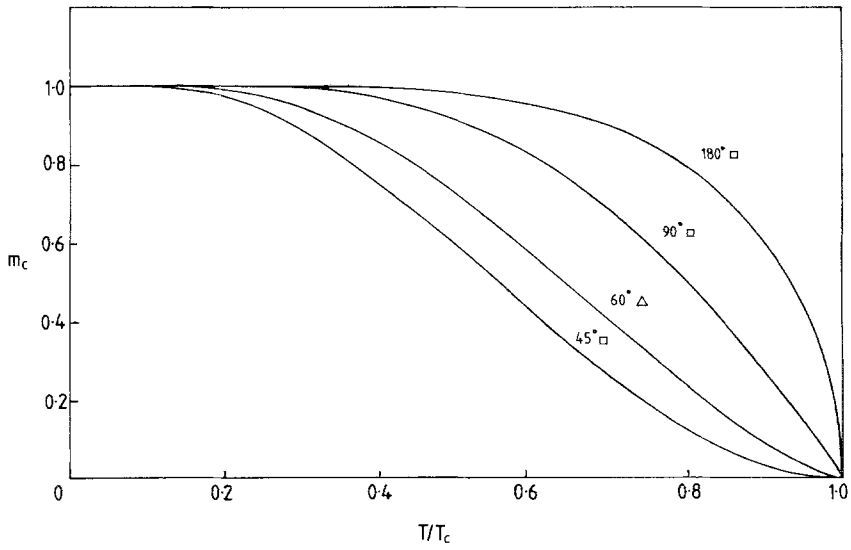

Fig. 5. Corner magnetization. All curves are for isotropic lattices, the lattices and wedge angle being indicated. The curve labeled (180° □) is the exact result for the surface magnetization.[11]

3. CRITICAL BEHAVIOR

Figure 5 already suggests that the corner magnetization exponent β_c defined by

$$m_c(T) \sim (1 - T/T_c)^{\beta_c}, \qquad T \to T_c - \tag{3.1}$$

depends upon the angle θ of the corner. More accurate estimates of β_c can be made if we make use of finite-size scaling to extrapolate $m_M(T_c)$, where T_c is the critical temperature of the relevant (triangular or square) lattice.

Finite-size scaling[12,13] asserts that if a thermodynamic quantity exhibits a singularity of the form (3.1) in the thermodynamic limit then for a finite system of linear dimension M

$$m_M(T_c) \sim AM^{-\beta_c/\nu}[1 + O(M^{-\omega})] \tag{3.2}$$

where ν is the bulk correlation length exponent and the correction term arises from the leading subdominant scaling field,[13,14] which is also responsible for (nonsingular) corrections[15] to (3.1).

For the $d = 2$ Ising model, $\nu = 1$. Hence we can estimate β_c from the limit of the sequence

$$b_M = M[1 - m_{M+1}(T_c)/m_M(T_c)] \to \beta_c \qquad \text{as } M \to \infty \tag{3.3}$$

Moreover, since it is believed[16] that there are no singular corrections in the $d = 2$ Ising model, one expects that[13,14,17] a finite lattice estimator such as b_M should have an asymptotic expansion of the form

$$b_M \approx \beta_c \left[1 + \sum_{j=1}^{\infty} c_j M^{-j}\right], \qquad M \to \infty \tag{3.4}$$

The $O(M^{-1})$ term is usually absent but arises here from the presence of free surfaces.[13]

The applicability of finite-size scaling and, in particular, the key results (3.2) and (3.4), to the corner magnetization is a crucial assumption for which we have no direct justification. Finite-size scaling and its predictions have been confirmed for *surface* quantities by exact calculations on the $d = 2$ Ising model[18] and the spherical model.[19] Our numerical results certainly support (3.4) and lead us to believe that this application of finite-size scaling ideas is also valid.

Table I lists values of b_M ($M \leqslant 50$) for the isotropic triangular lattice with a 60° corner. These data were obtained by iterating the recursion relation (2.20) from an initial lattice consisting of M rows of triangles with all couplings set to $K_c = \frac{1}{4} \ln 3 = 0.2747...$, the critical coupling of an infinite

Table I. Acceleration of Estimates for β_c for Isotropic Triangular Lattice with 60° Corner

		Accelerations		
M	b_M	alt-ε alg.	θ-alg.	u-transform
5	.86978	1.49317	1.50195	1.49930
10	1.13326	1.49949	1.49972	1.49986
15	1.24143	1.49993	1.49975	1.49995
20	1.30036	1.49999	1.49987	1.49998
25	1.33742	1.50001	1.49997	1.49999
30	1.36288	1.50000	1.49999	1.49999
35	1.38145	1.50000	1.50000	1.50000
40	1.39559	1.50000	1.50000	1.50000
45	1.40672			
50	1.41570			

triangular Ising model. For $M = 50$ this calculation involves in principle evaluating the partition function of 1250 spins, i.e., summing over more than 10^{350} configurations! The star–triangle recursion relation reduces this computational task to such an extent that all values of m_M for fixed K and $M = 2, 3,..., 50$ can be generated in less than 5 minutes on a UNIVAC 1108.

Despite this extensive range of lattice sizes, the sequence $\{b_M\}$ is very slowly convergent (see Table I). This convergence can, however, be improved by using standard sequence accelerators.[8,20] Previous applications[21] of such accelerators to finite-size scaling have been very successful with considerably less initial data than in this calculation. The actual accelerators we used are defined in Appendix B. The successive columns of Table I were obtained by

(i) one iteration of the alternating ε algorithm[20];

(ii) two iterations of the θ algorithm[8,10];

(iii) three iterations of Levin's u transform.[8,9]

Theoretically, these accelerators should be extremely efficient for sequences converging as in (3.4).[8,20] Table I shows that this does appear to be the case and suggests that

$$\beta_c(\pi/3) = 3/2 \tag{3.5}$$

is the exact exponent.

The other "simple" corners, namely, $\theta = 45°$ and 90° on the isotropic square lattice, can be handled in a similar way, the initial configurations of

coupling constants being given by (2.8) and (2.9), respectively, with $K = K_c = \frac{1}{2}\ln(1+\sqrt{2})$, the critical coupling of the square lattice Ising model. The results of the acceleration suggest that

$$\beta_c(\theta) = \pi/2\theta, \qquad \theta = \pi/4, \pi/3, \pi/2 \tag{3.6}$$

This result also reproduces the exactly known[11] surface magnetization exponent ($\beta_s = 1/2$) which corresponds to $\beta_c(\pi)$.

The same method can be applied to the *anisotropic* triangular lattice. In this case, the required values of m_M follow by iterating (2.20) for given M from an initial set of homogeneous couplings (K_1^c, K_2^c, K_3^c), where

$$\sinh 2K_1^c \sinh 2K_2^c + \sinh 2K_2^c \sinh 2K_3^c + \sinh 2K_3^c \sinh 2K_1^c = 1 \tag{3.7}$$

The resulting estimates of β_c for the special case $K_1^c = K_3^c$ are shown as a function of K_2^c in Fig. 6. The line in this figure is given by

$$\beta_c = (\pi/2)\arctan(1/\sinh 2K_2^c) \tag{3.8}$$

which actually reproduces the limiting estimates to better than four figures.

The expression (3.8) is also consistent with exponent estimates obtained for arbitrary anisotropy. In particular, (3.8) predicts for a 90° corner on an

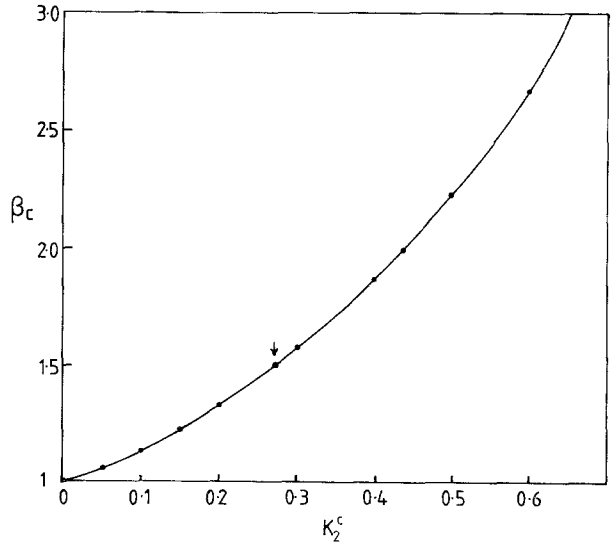

Fig. 6. Variation of the corner exponent β_c with K_2^c for an anisotropic triangular lattice with couplings $(K_1 = K_3, K_2)$. The points are the numerical estimates while the solid line is given by Eq. (3.8). The isotropic result is marked with an arrow.

anisotropic square lattice (obtained by setting $K_2 = 0$, $K_1 = K_1^c$, $K_3 = K_3^c$ with $\sinh 2K_1^c \sinh 2K_3^c = 1$) that $\beta_c = 1$ *independently* of the anisotropy. This conclusion has been verified numerically for a wide range of anisotropies.

4. EFFECTIVE ANGLES

We now present an argument which leads to the formula (3.8). Consider again a triangular lattice with arbitrary couplings K_1, K_2, K_3. The (bulk) correlations in this system will be anisotropic and in particular the three correlation lengths ξ_1, ξ_2, ξ_3 along the three axes will be different. From the expression for the spin correlation function given by Stephenson[22] one finds, for $T \leqslant T_c$,

$$\xi_1^{-1} = 2\left[\ln(\tanh K_1) + \operatorname{arcosh}\left(\frac{S_1 C_2 C_3 + C_1 S_2 S_3}{S_1}\right)\right] \tag{4.1}$$

where $C_i = \cosh 2K_i$, $S_i = \sinh 2K_i$ and ξ_2, ξ_3 follow by a permutation of the variables. As T approaches T_c, all ξ's diverge while their ratios go to finite limits given by

$$\xi_1 : \xi_2 : \xi_3 = \cosh 2K_1^c : \cosh 2K_2^c : \cosh 2K_3^c \tag{4.2}$$

Thus, increasing one coupling over the others leads to an increase of the corresponding correlation length. Note that these ξ's are dimensionless and correspond to a unit lattice constant in all three directions. One obtains proper physical quantities by setting $\bar{\xi}_i = \xi_i a_i$, where a_i are the real distances between spins. One can then make the $\bar{\xi}$'s equal by choosing the a's according to

$$a_1 : a_2 : a_3 = \frac{1}{\cosh 2K_1^c} : \frac{1}{\cosh 2K_2^c} : \frac{1}{\cosh 2K_3^c} \tag{4.3}$$

The correlations $\bar{\xi}_i$ are now isotropic, but the three principal directions no longer form 60° angles with each other. Denoting the angles opposite to a_i by θ_i^{eff}, one obtains, from the triangle formed by a_1, a_2, a_3

$$\sin\theta_1^{\text{eff}} : \sin\theta_2^{\text{eff}} : \sin\theta_3^{\text{eff}} = \frac{1}{\cosh 2K_1^c} : \frac{1}{\cosh 2K_2^c} : \frac{1}{\cosh 2K_3^c} \tag{4.4}$$

It follows that

$$\sin\theta_i^{\text{eff}} = \frac{A}{\cosh 2K_i^c} \tag{4.5}$$

where the constant A has to be determined from the sum rule $\theta_1^{\text{eff}} + \theta_2^{\text{eff}} + \theta_3^{\text{eff}} = \pi$. Using the criticality condition (3.7) this leads to $A = 1$ and (4.5) can be rewritten as

$$\theta_i^{\text{eff}} = \arctan\left(\frac{1}{\sinh 2K_i^c}\right), \qquad i = 1, 2, 3 \tag{4.6}$$

The θ_i^{eff} are the new angles between the principal directions of the lattice. We shall call them effective angles. A wedge with $\theta = 60°$ in the original system has an effective angle θ_i^{eff} in the transformed one, if K_i is the coupling across the wedge.

If one now assumes that in *any isotropic* system the corner exponent is given by the expression (3.5), then it follows immediately that for a 60° corner in an (originally) anisotropic system

$$\beta_c = \frac{\pi}{2\theta_i^{\text{eff}}} \tag{4.7}$$

This is exactly formula (3.8). Using the same reasoning, one can also treat larger angles. A wedge with $\theta = 120°$ can be decomposed into two adjacent 60° wedges. Each of them will be distorted differently under the rescaling, leading to two effective angles, say θ_1^{eff} and θ_2^{eff}. The corner exponent then is determined by their sum

$$\beta_c = \frac{\pi/2}{\theta_1^{\text{eff}} + \theta_2^{\text{eff}}} \tag{4.8}$$

This case includes again [as (4.7)] the square lattice with a 90° corner, if one sets $K_3 = 0$. Then $\theta_3^{\text{eff}} = \pi/2$ and consequently $\theta_1^{\text{eff}} + \theta_2^{\text{eff}} = \pi/2$, from which the already known result $\beta_c = 1$ follows. A final check is provided by treating a 180° corner, i.e., a straight surface. In this case we obtain

$$\beta_c = \frac{\pi/2}{\theta_1^{\text{eff}} + \theta_2^{\text{eff}} + \theta_3^{\text{eff}}} = \frac{1}{2} \tag{4.9}$$

which is again the well-known result.[11]

The effective angles have a simple physical interpretation. Consider again a 60° wedge: By increasing the coupling across the wedge, one couples the spins along this direction more strongly together. The system thereby becomes more one-dimensional. The angle θ^{eff} measures this effect in a simple geometric way and leads, via (4.7), to the expected result: β_c becomes larger and therefore m_c decreases, if the temperature is held fixed with respect to T_c.

5. CONICAL LATTICES

It is possible to convert corners or wedges of the square and triangular lattices into conical lattices by identifying the free edges radiating out from the corner spin. In many ways these conical lattices are simpler than their corresponding corners. One obvious simplification is that only *two* valences (apex and bulk) occur on conical lattices, whereas *three* valences (corner, edge, and bulk) occur on corner lattices. Despite such differences, one intuitively expects to see a close similarity between the behaviors of apex magnetizations and the corresponding corner magnetizations near the critical point. As we shall see this is indeed the case!

In this section we obtain the apex magnetizations of square and triangular conical lattices exactly using corner transfer matrix methods introduced by Baxter.[7,23,24] Following Tsang[25] we define a $2^M \times 2^M$ corner transfer matrix A, corresponding to the 60° wedge of the triangular lattice shown in Fig. 1, with elements

$$A(\boldsymbol{\sigma} \mid \boldsymbol{\sigma}') = \delta(\sigma_0, \sigma_0') \sum \exp H_M \tag{5.1}$$

Here $\boldsymbol{\sigma} = (\sigma_0, \sigma_1, ..., \sigma_{M-1})$ and $\boldsymbol{\sigma}' = (\sigma_0', \sigma_1', ..., \sigma_{M-1}')$ are the edge spins, the Kronecker delta ensures that the common apex spins $\sigma_0 = \sigma_0'$ match and the summation is over all interior spins of the corner. The Hamiltonian H_m is given by (2.6) with $\sigma(m, 0) = \sigma_m$, $\sigma(m, m) = \sigma_m'$, $K_1(m, 0) = 0$, and all other K's independent of m and n. The wedge is thus homogeneous except that the bonds on the right edge, as seen from the apex spin, are omitted. If the interactions K_1, K_2, K_3 are arranged as in Fig. 1, we will write

$$A = A(K_1, K_2, K_3) \tag{5.2}$$

The partition function for a conical lattice built up from a number of wedges is

$$Z = \operatorname{Tr} X \tag{5.3}$$

where X is a product of corner transfer matrices and the trace acts to join the first and the last edges. Similarly, the apex magnetization is given by

$$m_a = \operatorname{Tr} SX / \operatorname{Tr} X \tag{5.4a}$$

where

$$S(\boldsymbol{\sigma} \mid \boldsymbol{\sigma}') = \sigma_0 \delta(\sigma_0, \sigma_0') \, \delta(\sigma_1, \sigma_1') \cdots \delta(\sigma_{M-1}, \sigma_{M-1}') \tag{5.4b}$$

is the diagonal apex spin operator. Since the corner transfer matrix A breaks up into two diagonal blocks corresponding to $\sigma_0 = +1$ or -1, it commutes

with the matrix S for any K_1, K_2, and K_3. For isotropic interactions ($K_1 = K_2 = K_3 = K$), $X = A(K, K, K)^n$, where n is the number of wedges. In this case the apex angle is $\theta = n\pi/3$ and the apex magnetization is

$$m_a(n\pi/3) = \mathrm{Tr}\, SA^n / \mathrm{Tr}\, A^n \tag{5.4c}$$

where we have exhibited the dependence on the apex angle explicitly.

The corner transfer matrices of the triangular lattice have been diagonalized by Tsang.[25] To describe her results we parametrize the interactions as follows:

$$\cosh 2K_i = \mathrm{cnh}(2u_i, k), \qquad i = 1, 2, 3 \tag{5.5}$$

Here $\mathrm{cnh}(u, k) = \mathrm{cn}(iu, k)$ is a Jacobian elliptic function[7] of modulus k given by

$$k = \frac{(1 - t_1^2)(1 - t_2^2)(1 - t_3^2)}{4[(1 + t_1 t_2 t_3)(t_1 + t_2 t_3)(t_2 + t_3 t_1)(t_3 + t_1 t_2)]^{1/2}} \tag{5.6a}$$

with

$$t_i = \tanh K_i, \qquad i = 1, 2, 3 \tag{5.6b}$$

For ferromagnetic interactions ($K_1, K_2, K_3 \geqslant 0$) the elliptic parameters u_1, u_2, u_3 are nonnegative and satisfy the constraint

$$u_1 + u_2 + u_3 = I'/2 \tag{5.7}$$

where I, I' are the complete elliptic integrals of the first kind of moduli $k, k' = (1 - k^2)^{1/2}$, respectively. Notice that the moduli k, k' are unchanged by permuting the interactions K_1, K_2, and K_3.

As for the planar lattice, the critical point of the conical lattices occurs when $k = 1$ or $k' = 0$. In the ferromagnetic ordered phase of interest here, the moduli lie in $0 \leqslant k,\ k' \leqslant 1$. In the disordered phase $k \geqslant 1$ so that the modulus k is a temperaturelike variable. The parametrization (5.5) is well suited to low tempratures ($k \to 0$), but near criticality ($k' \to 0$) it is more convenient to use the equivalent conjugate modulus form:

$$\cosh 2K_i = 1/\mathrm{cn}(2u_i, k') \tag{5.8}$$

The nomes corresponding to k, k' are

$$q = \exp(-\pi I'/I), \qquad t = \exp(-\pi I/I') \tag{5.9}$$

respectively, where $0 \leqslant q,\ t \leqslant 1$. At low temperatures q goes to zero and t goes to one, whereas at criticality q goes to one and

$$t \sim 1 - k \sim T - T_c, \qquad T \to T_c - \tag{5.10}$$

Let us now introduce the additional variables

$$\omega_i = q^{1/4} \exp(\pi u_i/2I) = q^{\theta_i/2\pi}, \qquad i = 1, 2, 3 \tag{5.11}$$

where $0 \leqslant \theta_i \leqslant \pi/2$ and

$$\theta_i = \frac{\pi}{2} - \frac{\pi u_i}{I'}, \qquad i = 1, 2, 3 \tag{5.12}$$

the notation anticipating the identification of θ_i *at* T_c with an effective angle as in Section 4. Then Tsang[25] shows, using a suitable representation, that in the thermodynamic limit ($M \to \infty$)

$$S = \begin{pmatrix} 1 & 0 \\ 0 & -1 \end{pmatrix} \otimes \begin{pmatrix} 1 & 0 \\ 0 & -1 \end{pmatrix} \otimes \begin{pmatrix} 1 & 0 \\ 0 & -1 \end{pmatrix} \otimes \cdots \tag{5.13a}$$

and

$$A(K_1, K_2, K_3) = R(u_1)\, D(\omega_2)\, R(u_3)^{-1} \tag{5.13b}$$

where

$$D(\omega) = \text{const} \times \begin{pmatrix} 1 & 0 \\ 0 & \omega \end{pmatrix} \otimes \begin{pmatrix} 1 & 0 \\ 0 & \omega^3 \end{pmatrix} \otimes \begin{pmatrix} 1 & 0 \\ 0 & \omega^5 \end{pmatrix} \otimes \cdots \tag{5.13c}$$

and the R's are orthogonal matrices which commute with S and depend on only one of the u's as shown.

For isotropic interactions ($u_i = I'/6$), we see that $\theta_i = \pi/3$ and $\omega_i = q^{1/6}$. Putting this into (5.13) and (5.4c) we find that

$$m_a(\theta) = \prod_{r=1}^{\infty} \frac{1 - q^{(2r-1)\theta/2\pi}}{1 + q^{(2r-1)\theta/2\pi}} = P^2(q^{\theta/2\pi})/P(q^{\theta/\pi}) \tag{5.14a}$$

where

$$P(q) = \prod_{r=1}^{\infty} (1 - q^{2r-1}) \tag{5.14b}$$

and $\theta = n\pi/3$ is the apex angle. Clearly, the apex magnetization vanishes at criticality ($q = 1$). Also, setting $n = 6$, we regain the well-known result[26,27] for the bulk magnetization of the planar triangular lattice:

$$m_a(2\pi) = \prod_{r=1}^{\infty} \frac{1 - q^{2r-1}}{1 + q^{2r-1}} = (1 - k^2)^{1/8} \tag{5.15}$$

with a critical exponent $\beta_a(2\pi) = 1/8$.

To obtain the general critical behavior of the apex magnetization, we apply the conjugate nome transformation[7]

$$P(q^{\varepsilon}) \equiv \sqrt{2}\, q^{\varepsilon/24} t^{1/12\varepsilon} / P(t^{2/\varepsilon}) \tag{5.16}$$

From (5.14), we find that

$$m_a(\theta) = \sqrt{2}\, t^{\pi/4\theta} \prod_{r=1}^{\infty} \frac{(1 - t^{(2r-1)2\pi/\theta})}{(1 - t^{(2r-1)4\pi/\theta})^2} \tag{5.17}$$

It therefore follows that near the critical point ($t \to 0$)

$$m_a(\theta) \sim t^{\pi/4\theta} \sim (T - T_c)^{\pi/4\theta}, \qquad T \to T_c - \tag{5.18a}$$

and hence

$$\beta_a(\theta) = \pi/4\theta \tag{5.18b}$$

with $\theta = n\pi/3$. The fact that the angular dependence of this exponent appears in the denominator stems directly from the conjugate nome transformation (5.16).

It is now relatively straightforward to generalize these considerations to incorporate anisotropy of various forms. For example, for apex angles $\theta = n\pi$, we can consider the cone

$$X = [A(K_1, K_2, K_3) A(K_3, K_1, K_2) A(K_2, K_3, K_1)]^n \tag{5.19}$$

Using (5.4a), (5.11), (5.13) and the fact that

$$\theta_1 + \theta_2 + \theta_3 = \pi \tag{5.20}$$

we now obtain (5.14), (5.15), (5.17), and (5.18) with $\theta = n\pi$. So in this case these results are valid with *arbitrary* anisotropy.

Alternatively, if $K_1 = K_3 \neq K_2$, we can consider the cone

$$X = A(K_1, K_2', K_1)^n \tag{5.21}$$

In this case we have one degree of freedom θ_2 associated with the anisotropy where

$$\omega_2 = q^{\theta_2/2\pi}, \qquad 0 \leqslant \theta_2 \leqslant \pi/2 \tag{5.22}$$

This time the apex magnetization is given by (5.14) and (5.17) with $\theta = n\theta_2$ which is k dependent. However, the critical exponent β_a is given by (5.18)

with $\theta = n\theta_2^{\text{eff}}$ where θ_2^{eff} is the critical value of θ_2. But from (5.8) and (5.12), setting $k' = 0$ and $I' = \pi/2$, we have

$$\cosh 2K_2^c = 1/\cos 2u_2^c = 1/\sin \theta_2^{\text{eff}} \tag{5.23}$$

which is equivalent to the definition of effective angle given in (4.6). Hence, for a *single* wedge with an effective apex angle θ_2^{eff},

$$\beta_a = \frac{\pi}{4\theta_2^{\text{eff}}} = \frac{\pi}{4 \arctan(1/\sinh 2K_2^c)} \tag{5.24}$$

More generally, if

$$X = \prod_{i=1}^{n} A(K_{2i-1}, K_{2i}, K_{2i+1}) \tag{5.25}$$

where $K_{2n+1} = K_1$ and for each i the three interactions K_{2i-1}, K_{2i}, K_{2i+1} satisfy (5.6), then again β_a is given by (5.18b) if θ is the total effective apex angle given by

$$\theta = \sum_{i=1}^{n} \theta_{2i}^{\text{eff}} \tag{5.26}$$

The key results (5.14), (5.17), and (5.18) also hold for square lattices, which are obtained by setting one of the three interactions of the triangular lattice to zero. If we set $K_3 = 0$ in (5.6) we see that the modulus for square lattices is given by

$$k = (\sinh 2K_1 \sinh 2K_2)^{-1} \tag{5.27}$$

For isotropic interactions ($K_1 = K_2 = K$) we can take

$$X = A(K, 0, K)^n \tag{5.28}$$

or for anisotropic interactions we can take

$$X = [A(K_1, 0, K_2) A(K_2, 0, K_1)]^{n/2}, \qquad n \text{ even} \tag{5.29}$$

In both cases, the effective angle of each wedge is $\theta^{\text{eff}} = \pi/2$ and the total apex angle is $\theta = n\pi/2$, where n is the number of wedges.

Another way to obtain the square lattice is to take

$$X = [A(0, K_1, K_2) A(K_2, K_1, 0)]^n \tag{5.30}$$

This corresponds to n 90° corners of the square lattice where the axes of the corners project along the diagonals of the squares. In this case, the total

effective apex angle is $\theta = 2n\theta_1^{\text{eff}}$ so that the effective angle of each 90° corner lies between $0(K_1 \to \infty)$ and $\pi(K_1 \to 0)$. For $n = 1$, this gives

$$\beta_a = \frac{\pi}{8 \arctan(1/\sinh 2K_1^c)} \tag{5.31}$$

6. SQUARE LATTICE IN THE HAMILTONIAN LIMIT

In this section we return to a usual planar lattice and derive an exact expression for the magnetization at a 90° corner. The geometry is shown in Fig. 7. In order to simplify the calculation we shall consider the strongly anisotropic case (Hamiltonian limit) where $K_1 \ll K_2$. On the basis of our numerical results (Section 3) and the discussion of Section 4 we expect β_c for this geometry to be independent of the anisotropy and hence unaffected by the Hamiltonian limit. The row-to-row transfer matrix V is then given by $V = \exp(-K_2^* \mathscr{H})$, where K_2^* is the dual coupling of K_2 [$\tanh K_2^* = \exp(-2K_2)$] and $\mathscr{H}$ is the transverse Ising model Hamiltonian

$$\mathscr{H} = -\sum_{n=1}^{N} \sigma_n^z - \lambda \sum_{n=1}^{N-1} \sigma_n^x \sigma_{n+1}^x \tag{6.1}$$

Here σ_n^x, σ_n^z are Pauli matrices and $\lambda = K_1/K_2^*$ is the inverse of the parameter k, Eq. (5.27), evaluated for the present case. We shall study the case $T \leqslant T_c$ which corresponds to $\lambda \geqslant 1$. We also assume N to be even.

The corner magnetization can be extracted from the correlation function Γ_M between the spins at sites A and A'

$$\Gamma_M = \frac{\langle B | \sigma_1^x V^M \sigma_1^x | B \rangle}{\langle B | V^M | B \rangle} \tag{6.2}$$

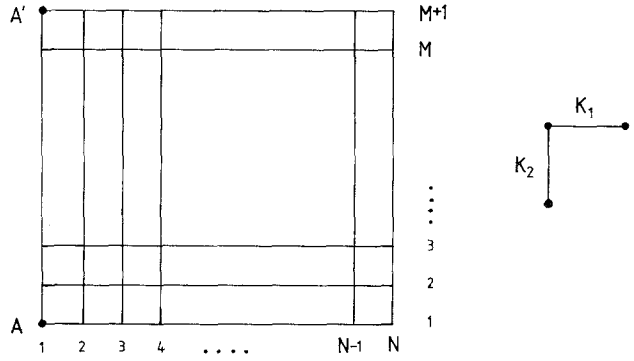

Fig. 7. Geometry of the square lattice used to evaluate m_c for a 90° corner by the row-to-row transfer matrix. Orientations of couplings K_1 and K_2 are shown.

where the state vector $|B\rangle$ describes the free summation over the boundary spins of the top and bottom row and is given explicitly by

$$|B\rangle = \prod_{n=1}^{N} \frac{1}{\sqrt{2}} [|\sigma_n^x = +1\rangle + |\sigma_n^x = -1\rangle]$$
$$= \prod_{n=1}^{N} |\sigma_n^z = +1\rangle \tag{6.3}$$

Comparison with $\mathscr{H}$ shows that $|B\rangle$ is the ground state of $\mathscr{H}$ *for* $\lambda = 0$. Therefore Γ_M is formally analogous to the correlation functions one encounters in the x-ray absorption problem.[28] The "time" evolution involves an operator $\mathscr{H}(\lambda)$ which is different from the operator $\mathscr{H}(\lambda = 0)$ to which the initial state belongs. Incidentally, such a relation with the x-ray problem also exists for the spin correlation functions in Ising lattices without free boundaries.[29] We also note that one row of horizontal couplings is missing from the expression (6.2) since our lattice contains $(M + 1)$ such rows. This is, however, a negligible effect in the present limit where $K_1 \ll 1$.

For large values of M, only the ground state $|0\rangle$ and the first excited state $|1\rangle$ of $\mathscr{H}$ are important in (6.2). The latter becomes degenerate with $|0\rangle$ for $N \to \infty$ and Γ_M goes to a finite limit, m_c^2, in this case. Therefore the corner magnetization is given, up to a sign, by

$$m_c = \frac{\langle 1 | \sigma_1^x | B \rangle}{\langle 0 | B \rangle} \tag{6.4}$$

where we have used that $|0\rangle$, $|B\rangle$ are even, while $|1\rangle$ is odd under the operator $P = \prod_n \sigma_n^z$. One now proceeds by writing $\mathscr{H}$ in terms of fermions

$$\mathscr{H} = -\sum_{n=1}^{N-1} (2c_n^+ c_n - 1) - \lambda \sum_{n=1}^{N-1} (c_n^+ - c_n)(c_{n+1}^+ + c_{n+1}) \tag{6.5}$$

and diagonalizes (6.5) by the standard procedure.[30,31] The result is, up to an additive constant,

$$\mathscr{H} = 2 \sum_q \varepsilon(q) \alpha_q^+ \alpha_q + 2\varepsilon(p) \alpha_p^+ \alpha_p \tag{6.6}$$

where q takes $(N - 1)$ values $0 < q < \pi$ and

$$\varepsilon(q) = (1 + \lambda^2 + 2\lambda \cos q)^{1/2} \tag{6.7}$$

The quantity $\varepsilon(p)$ is of order λ^{-N} and therefore vanishes for $N \to \infty$. Thus the state $|0\rangle$ is the vacuum state of the Fermi operators α and the state $|1\rangle$ is

given by $|1\rangle = \alpha_p^+ |0\rangle$. Finally, the canonical transformation relating the old and new Fermi operators is

$$c_n = \sum_{k=q,p} [g_{kn}\alpha_k + h_{kn}\alpha_k^+] \tag{6.8}$$

where g and h, together with some further details, are given in Appendix C.

We now insert $\sigma_1^x = c_1^+ + c_1$ into (6.4) and use (6.8) together with the relations

$$\alpha_q |0\rangle = \alpha_p |0\rangle = 0 \tag{6.9a}$$

$$\alpha_q |1\rangle = 0, \qquad \alpha_p |1\rangle = |0\rangle \tag{6.9b}$$

This leads to the formula

$$m_c = \phi_p(1) + \sum_q \phi_q(1) f_q \tag{6.10}$$

where $\phi = g + h$, see (C.8), and

$$f_q = \frac{\langle 1 | \alpha_q | B \rangle}{\langle 0 | B \rangle} \tag{6.11}$$

In order to determine f_q we follow Abraham[32] and use the identities

$$c_n^+ |B\rangle = 0, \qquad n = 1, 2, \ldots, N \tag{6.12}$$

in the form $\langle 1 | c_n^+ | B \rangle = 0$. Inserting (6.8) again, this gives the set of N equations:

$$\sum_q f_q h_{qn} = -g_{pn}, \qquad n = 1, 2, \ldots, N \tag{6.13}$$

Because the functions g_{qn}, h_{qn} are either symmetric or antisymmetric under a reflection $n \to N + 1 - n$ (see Appendix C), the system (6.13) can be split into two systems.

(*a*) *Symmetric functions, $N/2$ values of q (denoted by q_1)*:

$$\sum_{q_1} f_q h_{qn} = -g_{pn}, \qquad n = 1, 2, \ldots, \frac{N}{2} \tag{6.13a}$$

(*b*) *Antisymmetric functions, $(N/2 - 1)$ values of q (denoted by q_2)*:

$$\sum_{q_2} f_q h_{qn} = 0, \qquad n = 1, 2, \ldots, \frac{N}{2} \tag{6.13b}$$

Therefore, unless the h_q are linearly dependent (which we assume not to be the case) (6.13b) leads to $f_q = 0$ for the q_2 values and (6.13a) uniquely determines the remaining f's.

Now we use the explicit form of h_{qn} for the q_1 values

$$h_{qn} = \frac{1}{2} C_q \frac{\cos[q(n-L)]}{\cos[qL]} \tag{6.14}$$

where $L = (N+1)/2$ is the coordinate of the centre of the spin chain, and form the overlap matrix

$$S_{qq'} = \sum_{n=1}^{N/2} \frac{\cos[q(n-L)]\cos[q'(n-L)]}{\cos[qL]\cos[q'L]} \tag{6.15}$$

The result is, after some manipulations,

$$S_{qq'} = -\frac{1}{2}\left[1 + \frac{\tan(qL)\sin q - \tan(q'L)\sin q'}{\cos q - \cos q'}\right], \qquad q \neq q' \tag{6.16a}$$

$$S_{qq} = \frac{1}{2}\frac{N + \varepsilon(q)^{-1}}{1 + \cos(2qL)}, \qquad q = q' \tag{6.16b}$$

One can eliminate the quantity L by inserting the relations

$$\tan(qL) = -\frac{\varepsilon(q) + 1 + \lambda\cos q}{\lambda \sin q} \tag{6.17a}$$

$$\cos(2qL) = -\frac{1 + \lambda\cos q}{\varepsilon(q)} \tag{6.17b}$$

which follow from the equations determining the q_1 values. Then (6.16a) becomes simply

$$S_{qq'} = \frac{1}{2}\frac{1}{\varepsilon(q) + \varepsilon(q')}, \qquad q \neq q' \tag{6.18}$$

In the same way one calculates the overlap of the function g_p with $h_{q'}$, leading to

$$G_{q'} = \sum_{n=1}^{N/2} (-1)^n \lambda^{-n} \frac{\cos[q'(n-L)]}{\cos[q'L]}$$

$$= \frac{1}{\varepsilon(q')} \qquad \text{for } N \gg 1 \tag{6.19}$$

Equation (6.13a) can therefore be written as

$$\sum_{q_1} F_q S_{qq'} = -G_{q'} \tag{6.20}$$

where $F_q = f_q C_q / C_p$. Finally, we take the limit $N \to \infty$ by going over from sums to integrals, using $N\delta_{qq'} = 2\pi\delta(q - q')$. In this way we arrive at the integral equation of Fredholm type

$$F(q)\frac{\varepsilon(q)}{\varepsilon(q) - (1 + \lambda \cos q)} + \int_0^\pi \frac{dq'}{\pi} \frac{F(q')}{\varepsilon(q) + \varepsilon(q')} = -\frac{1}{\pi\varepsilon(q)} \tag{6.21}$$

In terms of $F(q)$ the corner magnetization is then given as

$$m_c = \left(1 - \frac{1}{\lambda^2}\right)^{1/2} \left[1 + \int_0^\pi dq\, F(q)\right] \tag{6.22}$$

Equations (6.21) and (6.22) contain the solution of the problem. It remains to determine $F(q)$ from the integral equation. While a closed form solution is hard to obtain, one can easily find $F(q)$ as a power series in $1/\lambda$ by expanding all quantities in this parameter. This corresponds to a low-temperature expansion of m_c. The first approximation is, for example,

$$F(q) = -\frac{1}{\pi\lambda}(1 - \cos q) \tag{6.23}$$

In this way one finds, through order $1/\lambda^3$

$$\begin{aligned} m_c &= \left(1 - \frac{1}{2\lambda^2}\right)\left(1 - \frac{1}{\lambda} + \frac{1}{2\lambda^2} - \frac{1}{2\lambda^3}\right) \\ &= 1 - \frac{1}{\lambda} + O\left(\frac{1}{\lambda^4}\right) \end{aligned}$$

From this one suspects that

$$m_c = 1 - \frac{1}{\lambda} \tag{6.24}$$

is the exact result to all orders. This result for m_c is also supported by direct numerical calculations based on (6.13a) and (6.10). Thus we have found a very simple law for m_c and, at the same time, confirmed the value $\beta_c = 1$ for a 90° corner in this highly anisotropic lattice.

Finally, let us compare this result with the formulas for the surface magnetization. They can be obtained either from the general expressions of

McCoy and Wu[11] or also directly within the present Hamiltonian approach. For example, to obtain m_s on a horizontal surface, one does the same calculation as above, but with a *cyclic* Hamiltonian. This leads to some interesting changes caused by the translational invariance. The equations analogous to (6.13) in this case do not specify all necessary matrix elements since one of the functions h_q is zero. At the same time, however, the states $|0\rangle$ and $|1\rangle$ are simple product wave functions of BCS type so that the remaining matrix elements $\langle 1|\alpha_\pi|B\rangle$ and $\langle 0|B\rangle$ can be evaluated directly. The result is

$$m_{s,h} = (1 - 1/\lambda)^{1/2} \tag{6.25}$$

On the other hand, for a spin on a vertical surface, one simply has to replace $|B\rangle$ by $|0\rangle$ in (6.4) and finds[31]

$$m_{s,v} = (1 - 1/\lambda^2)^{1/2} \tag{6.26}$$

Both laws are not identical since in the first case the couplings in the surface are weak, while in the second case they are strong. However, as for the corner magnetization, the critical exponent $\beta_s = 1/2$ is not affected by the anisotropy.

7. SUMMARY AND CONCLUSION

In this paper we have used a variety of methods to study the critical behavior of the corner or apex magnetization of two-dimensional Ising models in wedge-shaped domains. The domains either have free edges or are wrapped on a cone (conical boundary conditions). The main conclusions of this work are as follows:

(i) for isotropic systems with free edges

$$\beta_c = \pi/2\theta \tag{7.1}$$

where θ is the opening angle of the wedge;

(ii) for isotropic conical lattices

$$\beta_a = \pi/4\theta \tag{7.2}$$

(iii) for an anisotropic triangular lattice these results remain valid with θ replaced by

$$\theta^{\text{eff}} = \arctan(1/\sinh 2K_2^c) \tag{7.3}$$

where K_2 is the coupling across the wedge or cone (recall Fig. 1). For conical lattices these results were established analytically by the use of corner transfer matrices. For free edge conditions (7.1) is a conjecture, albeit one that is impressively supported by numerical calculations.

The most striking features of these results is the ubiquitous ratio

$$\beta_c : \beta_a = 2 : 1 \tag{7.4}$$

for which we have no explanation. In this connection, a comparison of the temperature dependences of the corner and apex magnetizations is interesting. This is done in Fig. 8 for a 90° corner in an isotropic square lattice. Rather surprisingly m_a is less than m_c except near T_c, whereas naively, on the basis of the Griffiths' inequalities,[33] one might expect m_a to exceed m_c at all temperatures. The reason for this behavior is, however, easy to understand. Closing the free wedge onto itself only yields the homogeneous conical geometry if interactions along the boundaries of the wedge are halved. If this is done, the resulting magnetization (see Fig. 8) does indeed lie below the cone result. Such a modification of the interactions, apparently, does not affect the exponent β_c, a conclusion we have confirmed by the numerical methods of Section 3.

Our discussion in Section 4 of the decay of correlations in anisotropic lattices helps to unravel the way the anisotropy enters explicitly into the

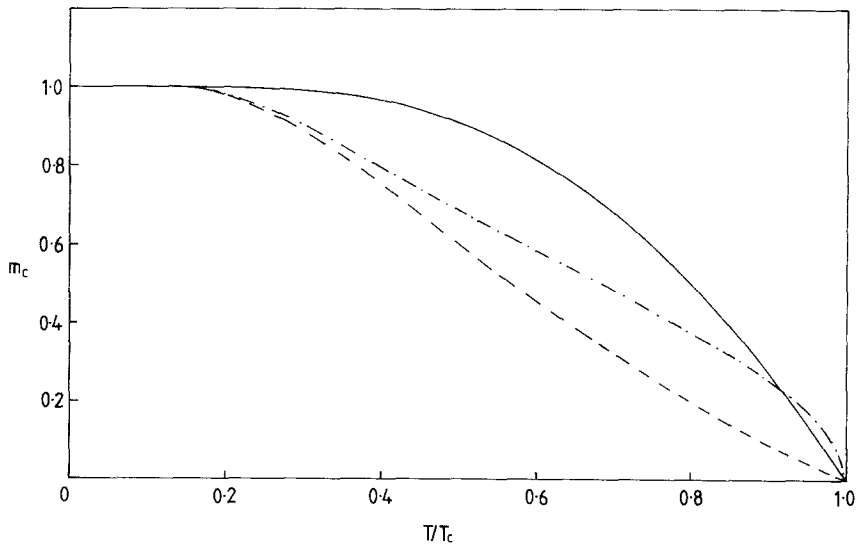

Fig. 8. Comparison of corner magnetization for 90° wedge with free boundaries (——) conical boundary condition (—· — ·), and free boundaries with the edge coupling reduced by a factor of 2 (– – –).

magnetization exponents. This mechanism is the same as Cardy[1] conjectured would occur for a continuum field theory. The necessary rescaling to recover an *isotropic* lattice in general distorts angles.

No distortion occurs for $\theta = \pi$ where $\beta_c = \beta_s = 1/2$, or for $\theta = \pi/2$ where $\beta_c = 1$ provided in this case the 90° angle is constructed with the edges along lattice vectors of a square lattice. However, if one rotates the wedge so that the axes project along the diagonals of the square, the exponent should depend upon the anisotropy. While we are unable to probe this geometry directly with free edges, it can be handled with conical boundary conditions; the resulting expression for β_a being given in (5.31). Assuming that (7.4) is valid implies for free edges that

$$\beta_c = \frac{\pi}{4 \arctan(1/\sinh 2K_1^c)}$$

K_1 being the coupling across the wedge.

Finally, it should be noted that setting $\theta = 2\pi$ for a wedge with free edges does *not* yield the bulk magnetization exponent. Instead, we obtain a lattice with a "cut" in it and $\beta_c(2\pi) = 1/4$.

Our calculations could be extended in several directions. Conical lattices could be considered for the eight-vertex model again using corner transfer methods. We have noted that the corner exponent does not appear to be affected by modifying the interaction in the edge. More complex inhomogeneities in which the couplings approach their bulk values only as one moves away from the edge and/or the corner could have more drastic effects as seen in the surface case.[5,6] The star–triangle recursion method of Section 3 may be able to handle this case, but these possibilities are beyond the scope of this paper.

APPENDIX A: STAR–TRIANGLE TRANSFORMATION

The star–triangle transformation is illustrated in Fig. 3a. Summing over the configurations of the spin at the central node of the star gives

$$K_i = F(p_i, p_j, p_k), \qquad (i, j, k) \text{ cyclic} \tag{A.1}$$

where

$$F(p, p', p'') = \frac{1}{4} \ln \left[\frac{\cosh(p + p' + p'') \cosh(-p + p' + p'')}{\cosh(p - p' + p'') \cosh(p + p' - p'')} \right] \tag{A.2}$$

and we have suppressed the spatial dependence of the K's and p's. To obtain the inverse transformation, $p_i = p_i(K_1, K_2, K_3)$ define[3] (i, j, k, cyclic)

$$u_i = \sinh 2K_j \sinh 2K_k, \qquad v_i = 1/\sinh 2p_j \sinh 2p_k \tag{A.3}$$

then the star–triangle transformation becomes[3]

$$v_i = k^2(u)u_i, \qquad u_i = k^2(v)v_i \tag{A.4}$$

where

$$k^{-2}(x) = x_1^2 + x_2^2 + x_3^2 + 2x_1x_2x_3 + 2[(x_1 + x_2x_3)(x_2 + x_3x_1)(x_3 + x_1x_2)]^{1/2} \tag{A.5}$$

and

$$k^2(u) = k^{-2}(v) \tag{A.6}$$

Hence from (A.4)

$$\sinh 2p_i = k^{-1}(u)/\sinh 2K_i \tag{A.7}$$

Since we wish to allow for zero couplings, it is computationally advantageous to define

$$y_i = e^{-2p_i} \tag{A.8}$$

where from (A.6)

$$y_i = \frac{k(u)\sinh 2K_i}{1 + [1 + k^2(u)\sinh^2 2K_i]^{1/2}}, \qquad i = 1, 2, 3 \tag{A.9}$$

This equation together with (A.2) form the basis of our iteration of (2.13) and hence (2.20) for m_M.

APPENDIX B: CONVERGENCE ACCELERATORS

In this appendix we define the convergence accelerators used in Sections 3 and 4. A convergence accelerator for a given sequence $\{f_n^{(0)}\}_{n=0}^{N_0}$ consists[8] of a (nonlinear) transformation of the sequence to yield a new sequence $\{f_n^{(1)}\}_{n=0}^{N_1}$ such that

$$\lim_{n\to\infty} f_n^{(0)} = \lim_{n\to\infty} f_n^{(1)} = f_\infty \tag{B.1}$$

and

$$\lim_{n\to\infty} \left| \frac{f_\infty - f_n^{(1)}}{f_\infty - f_n^{(0)}} \right| = 0 \tag{B.2}$$

In principle further acceleration can be achieved by reapplying the accelerator to $\{f_n^{(1)}\}$ to obtain $\{f_n^{(2)}\}$ etc. In practice, the number of iterations is limited by two factors:

(i) $N_1 < N_0$, so that each application reduces the number of terms available;

(ii) round-off error tends to build up due to the finite precision arithmetic of a computer.

The three accelerations used in this paper are defined as follows:

(i) θ algorithm[8,10]:

$$\theta_n^{(k)} = \theta_n^{(k-1)} + 1/\Delta f_n^{(k)} \tag{B.3a}$$

$$f_n^{(k+1)} = f_{n+1}^{(k)} + \Delta f_{n+1}^{(k)} \Delta\theta_{n+1}^{(k)}/\Delta^2\theta_n^{(k)} \tag{B.3b}$$

with $\theta_n^{(-1)} = 0$;

(ii) alternating ε algorithm[20,21]:

$$\varepsilon_n^{(2k+1)} = \alpha_k \varepsilon_n^{(2k-1)} + 1/\Delta\varepsilon_n^{(2k)} \tag{B.4a}$$

$$\varepsilon_n^{(2k+2)} = \varepsilon_n^{(2k)} + 1/\Delta\varepsilon_{n-1}^{(2k+1)} \tag{B.4b}$$

$$f_n^{(k)} = \varepsilon_n^{(4k)} \tag{B.4c}$$

with $\varepsilon_n^{(-1)} = 0$, $\varepsilon_n^{(0)} = f_n^{(0)}$, and $\alpha_k = [(-)^k - 1]/2$;

(iii) u transform[8,9]:

$$f_n^{(k)} = \Delta^k(f_n^{(0)} C_n^{(k)})/\Delta^k C_n^{(k)} \tag{B.5a}$$

$$C_n^{(k)} = n^{k-1}/n\Delta f_n^{(0)} \tag{B.5b}$$

where, in (B.3)–(B.5),

$$\Delta x_n = x_{n+1} - x_n \tag{B.6}$$

APPENDIX C

To diagonalize $\mathscr{H}$ in Eq. (6.5) one has to find the eigenfunctions of the $(N \times N)$ matrix

$$(A-B)(A+B) = 4\begin{pmatrix} 1 & \lambda & & & \\ \lambda & 1+\lambda^2 & \lambda & & \\ & & \ddots & & \\ & & & & \lambda \\ & & & \lambda & 1+\lambda^2 \end{pmatrix} \tag{C.1}$$

where we follow the notation of Lieb, Schultz, and Mattis.[30] The wavelike solutions are

$$\phi_q(n) = C_q \left[\cos(qn) - \frac{1 + \lambda \cos q}{\lambda \sin q} \sin(qn) \right] \tag{C.2}$$

where the q values follow from

$$\frac{\sin[q(N+1)]}{\sin(qN)} = -\lambda \tag{C.3a}$$

or, equivalently, from

$$\tan[q(N+1)] = \frac{\lambda \sin q}{1 + \lambda \cos q} \tag{C.3b}$$

and C_q is the proper normalization factor. For $\lambda > 1$ there is, in addition, an oscillating exponential solution

$$\phi_p(n) = C_p(-1)^n [e^{-pn} - e^{p(n-2N-2)}] \tag{C.4}$$

where, for $N \to \infty$, $e^p = \lambda$ and $C_p = (\lambda^2 - 1)^{1/2}$.

In addition to the functions ϕ one needs the functions ψ, which are the eigenfunctions of $(A+B)(A-B)$. They are simply related to the ϕ's since $(A+B)(A-B)$ is obtained by a reflection $n \to N+1-n$ from $(A-B)(A+B)$. It is convenient to distinguish two kinds of q values, namely,

(a) Solutions of (C.3) with $\sin(qN) > 0$ (q_1 values):

Then
$$\psi_q(n) = -\phi_q(N+1-n) \tag{C.5}$$

(b) Solutions of (C.3) with $\sin(qN) < 0$ (q_2 values):

Then
$$\psi_q(n) = +\phi_q(N+1-n) \tag{C.6}$$

For N even, also the p state belongs to this class

$$\psi_p(n) = +\phi_p(N+1-n) \tag{C.7}$$

The functions g, h in (6.8) are given by

$$g_{kn} = \tfrac{1}{2}[\phi_k(n) + \psi_k(n)] \qquad k = q, p \tag{C.8a}$$

$$h_{kn} = \tfrac{1}{2}[\phi_k(n) - \psi_k(n)] \tag{C.8b}$$

Therefore in class (a) g is antisymmetric and h is symmetric, while in class (b) the symmetries are interchanged. Note the special cases

$$\phi_q(1) = -\frac{1}{\lambda} C_q$$

$$\phi_p(1) = -\frac{1}{\lambda} C_p = -\left(1 - \frac{1}{\lambda^2}\right)^{1/2}$$

which appear in the expression (6.10) for m_c. The expression (6.14) for h_{qn} is easily derived from (C.2) and (C.5).

NOTE ADDED IN PROOF

It is possible (Barber, unpublished; Cardy, to be published) to relate the corner exponents to standard surface exponents by the use of the conformal invariance of correlation functions at criticality. This argument predicts that

$$\beta_c = (\pi/\theta)\beta_1$$

which is consistent with our result (3.6). The surface exponents in turn can be expressed (Cardy, to be published) in terms of the bulk correlation length exponent ν. Explicitly, his results are $\beta_1 = \nu/(3\nu - 1)$ for the q-state Pott's model ($0 < q < 4$) and $\beta_1 = \nu(2\nu + 1)/2(4\nu - 1)$ for $O(n)$-models ($0 \leqslant n < 2$). The resulting prediction of the corner exponents for $n = 0$ has been confirmed by a direct study of self-avoiding walks in two-dimensional wedges (Guttmann and Torrie, to be published; Cardy and Redner, to be published).

A similar application of conformal invariance predicts (Cardy, private communication) that the *apex* magnetization exponent is given by

$$\beta_a = (2\pi/\theta)\beta$$

so that $\beta_c : \beta_a = \beta_1 : 2\beta$, which yields (7.4) in the Ising case.

REFERENCES

1. J. H. Cardy, *J. Phys. A* **16**: 3617 (1983).
2. See, e.g., W. Panofsky and M. Phillips, *Classical Electricity and Magnetism*, (Addison-Wesley, Cambridge, 1955), Section 4.11.
3. I. Syozi, in *Phase Transitions and Critical Phenomena*, C. Domb and M. S. Green, eds. (Academic Press, London, 1972), Vol. 1, p. 270.

4. H. J. Hilhorst, M. Schick, and J. M. J. van Leeuwen, *Phys. Rev. B* **19**:2749 (1979).
5. H. J. Hilhorst and J. M. J. van Leeuwen, *Phys. Rev. Lett.* **47**:1188 (1981).
6. T. W. Burkhardt and I. Guim, *Phys. Rev. B* **29**:508 (1984).
7. R. J. Baxter, *Exactly Solved Models in Statistical Mechanics* (Academic Press, London, 1982).
8. D. A. Smith and W. F. Ford, *SIAM J. Numer. Anal.* **16**:223 (1979).
9. D. Levin, *Internat. J. Comput. Math. Ser. B* **3**:371 (1973).
10. C. Brezinski, *C.R. Acad. Sci. Paris Sér. A-B* **273**:A727 (1971).
11. B. M. McCoy and T. T. Wu, *Phys. Rev.* **162**:436 (1967).
12. M. E. Fisher and M. N. Barber, *Phys. Rev. Lett.* **28**:1516 (1972).
13. M. N. Barber, in *Phase Transitions and Critical Phenomena*, C. Domb and J. L. Lebowitz, eds. (Academic Press, London, 1983), Vol. 8, p. 146.
14. V. Privman and M. E. Fisher, *J. Phys. A* **16**:L295 (1983).
15. F. J. Wegner, *Phys. Rev. B* **5**:4529 (1972).
16. A. Aharony and M. E. Fisher, *Phys. Rev. Lett.* **45**:679 (1980).
17. M. N. Barber, to be published.
18. H. Au-Yang and M. E. Fisher, *Phys. Rev. B* **11**:3469 (1975).
19. M. N. Barber, *J. Stat. Phys.* **10**:59 (1974).
20. M. N. Barber and C. J. Hamer, *J. Austral. Math. Soc. (Ser. B)* **23**:229 (1982).
21. C. J. Hamer and M. N. Barber, *J. Phys.* **A14**:2009 (1981).
22. J. Stephenson, *J. Math. Phys.* **11**:420 (1970).
23. R. J. Baxter, *J. Stat. Phys.* **15**:485 (1976); **17**:1 (1977).
24. R. J. Baxter, *Physica* **106A**:18 (1981).
25. S. K. Tsang, *J. Stat. Phys.* **17**:137 (1977).
26. H. S. Green, *Z. Phys.* **171**:129 (1963).
27. R. B. Potts, *Phys. Rev.* **88**:352 (1952).
28. See G. D. Mahan, *Many Particle Physics* (Plenum Press, New York and London, 1981).
29. I. Peschel and K. D. Schotte, *Z. Phys.* **B54**:305 (1984).
30. E. H. Lieb, T. D. Schultz, and D. C. Mattis, *Ann. Phys. (N.Y.)* **16**:406 (1961).
31. P. Pfeuty, *Ann. Phys. (N.Y.)* **57**:79 (1970).
32. D. B. Abraham, *Commun. Math. Phys.* **59**:17 (1978); Eq. (2.43).
33. R. B. Griffiths, in *Phase Transitions and Critical Phenomena*, C. Domb and M. S. Green, eds. (Academic Press, London, 1972), Vol. 1, p. 7.